Nano LIFE
(2023) 2330005 (21 pages)

DOI: 10.1142/S1793984423300054

Taming of Organic Pollutants Using Covalent-Organic-Framework-Based Materials: Challenges and Future Prospects

Jasvinder Kaur*,§, Vivek Sharma† and Ram K. Gupta‡
*Department of Chemistry, School of Sciences
IFTM University, Moradabad, Uttar Pradesh 244102, India
†Department of Chemistry, GLA, University, Mathura
Uttar Pradesh 281406, India
‡Department of Chemistry, Pittsburg State University
Pittsburg, KS 66762, USA
§jasvinderkaur2911@gmail.com

Received 24 April 2023
Accepted 18 June 2023
Published 5 August 2023

Being available in water and air, organic contaminants have easy access to animal bodies to accumulate in the biological food chain, resisting chemical, biological, and photolytic degradation. Besides, they have the ability to travel great distances to end up being dispersed across a broad area, even in places where they have never been used. Furthermore, they pose a significant risk to both human society and the environment, which forces the international scientific community to plan and act to eradicate organic pollutants from the environment and establish a mechanism to stop their discharge. In this context, covalent organic frameworks (COFs)-based materials are found to be promising to control air and water pollutants because of their unique porous, and polymeric crystal structure. This study highlights the history, design, and applications of COFs for reducing organic pollution, as well as the obstacles and opportunities facing their widespread usage in environmental remediation today.

Keywords: Covalent organic frameworks; environmental remediation; organic pollutants.

1. Introduction

1.1. *Importance of taming of organic pollutants*

Organic pollutants (OPs) are composed of toxic ingredients based on carbonaceous compounds and their increasing release and disposal have already become a serious threat to living and the environmental kingdom. Moreover, their long-time stability in the environment is creating an even greater threat. Being recalcitrant and lipophilic in nature, they affect greatly humans and wildlife by getting accumulated in fatty tissues of creatures and staying there for long time.[1] It is assumed that around 90% of human beings get exposed to Ops in one way or the other, causing health hazards. A lot of investigations related to its response to photocatalytic oxidation have been done and are still going on in search of an effective strategy to combat OPs. A black list of OPs has been prepared based on

§Corresponding author.

their gravity of harmful effect following the diplomatic signature of the stockhom convention. Aldrin, dichlorodiphenyltrichloroethane (DDT), dieldrin, endrin, heptachlor, chlordane, murex, and toxaphene hexachlorobenzene and polychlorinated biphenyls (PCBs), polychlorinated dibenzodioxins (PCDDs) and polychlorinated dibenzofurans (PCDFs) are dominating members in the list.[2] High proclivity for biomagnification in food chain, linked to carcinogenic and endocrine effects, make these compounds hazardous.[3] An examination of human adipose tissues from Europe, Africa, Asia revealed the existence of OP residue. Toxic components of pesticides on long time persistence are observed to be more lethal for killing targeted microorganisms bringing problem for humans and environment simultaneously. For instance, dichlorodiphenyldichloroethanes (DDEs), a derivative of DDT, have long half-life and get accumulated in adipose tissues of humans posing severe health risk. DDT metabolism may release DDE or DDE possessing food staffs.[4] However, when clarity of scientific information is inadequate, any empirical decision is monitored nationally or internationally due to uncertainty of detrimental effects on environment, therefore, elaborate research and development ought to be done to detect health issues along with their possible solution on a priority basis. Now, it is well understood by scientific community about the severity of OPs, and how dangerous these OPs can be for the generations to come. Increasing industrial development takes OPs pollution to environment simultaneously will lead to deadly consequences, including oxidative stress along with cell death. Although developed countries like USA and Europe have planned to eliminate OPs from environment completely, developing countries are far behind even to offer an effective thought to plan and execute suitable strategy to eradicate of OPs from nature. In this context, electrochemical and photochemical strategies have been considered as fascinating approaches for the taming of OPs, requiring efficient catalytic materials.

1.2. *Expectations from covalent organic frameworks for organic pollutants taming*

The COFs are considered an emerging type of functional nanostructures possessing interesting characteristics because of the exploitable combined effect of high crystallinity, large surface and adjustable pore size along with unique molecular structure for various applications from energy to environment. During recent times, a lot of investigations involving novel strategies have been carried out to treat Ops,[1,5] and COFs-based approaches, out of all these protocols, have been recently studied for taming of OPs, because they possess properties suitable for treatment of Ops: (i) extended surface area along with pore volume and high sorption ability, (ii) availability of active sites to accommodate OPs chemisorption and/or degradation; (iii) cavities suitable to undergo functionalization for host–guest interaction; (iv) possibility of COFs tailoring[6]; (v) possibility of large-scale production of COFs as well as the chance of shaping them as monoliths, pellets, membranes, or columns, being used for the decontamination machines (Fig. 1).

The aim of using COFs is to address multiple environmental issues simultaneously like selective adsorption of OPs on COFs, which provides a platform to undergo catalytic degradation of OPs. Modification of COFs can be achieved via monitoring pore diameter or by making COF composites with enhanced absorbing and/or catalytic abilities for treatment of OPs. Moreover, although the use of COFs has been reported in a wide variety of contexts, including gas storage,[7,8] and various other fields,[9,10] due to the advantages associated with their stability in aqueous media, even under extreme conditions, however, how they might be used to control organic pollutants is seldom reported. Therefore, this review article is written to shed light on how COFs can be used to clean up the environment to help humans living free of organic pollutants. As such, this review's primary objective is to present a fresh perspective on several classes of COF-based materials having potential usefulness. Lastly, the key potential challenges and future perspectives are also discussed in detail.

2. Science and Synthesis Approaches for Covalent Organic Frameworks

Linking of properties and suitability of porous materials is made based on size shape, arrangement, and porosity along with the composition of material.[11] Scientists are well engaged in this area to manipulate composition along with structure of porous material which is responsible for determining the control and functionality of the internal surface of porous materials. Modular construction utilizing molecular

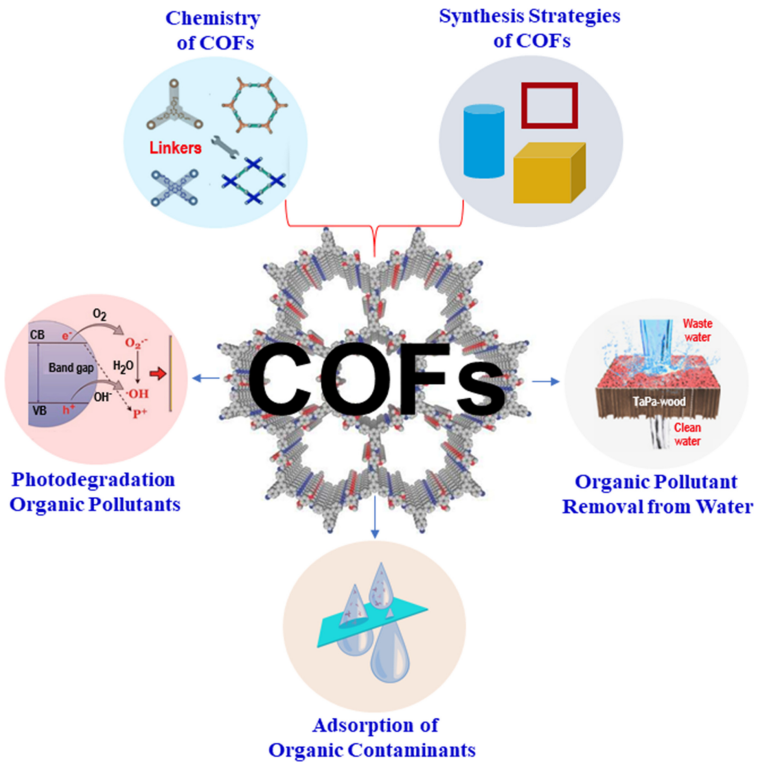

Fig. 1. A systematic representation of COFs features and their applications in OP taming.

components is a remarkable recent development that can be connected to adjoin sub-unit,[12] which led to receiving an outstanding porous material like COFs, having carbon and other elements covalently bonded open network.[13] with precise control on structure and composition. Independent tuning of pore geometries as well as functionalities is offered by modular nature of this material, which allows to compare and develop connectivity among parameters individually. Application of cost-effective and eco-friendly porous material to tame organic pollutants is a research in demand, by manipulating their structure and function in order to improve their activities. COFs appear to be the candidate of choice to address all challenges related to environment remediation, sustainability along with Ops treatment. In the following sub-sections, we explored the science and engineering of COFs and how to alter their features for OPs taming.

2.1. *Chemistry of covalent organic frameworks*

The main challenge involved in extension of MOF network to covalently bonded polymer is the extremely strong bond strength of many organic functional groups, which do not participate in dynamic exchange process like coordination complexes. Therefore, organic molecules bonded covalently with extended solid yield amorphous, disordered material.[14] Crystalline morphology was obtained by drawing balance kinetics and thermodynamic reversibility of the reaction as revealed by Yaghi *et al.*[15] who introduced the first two COF members. 1,4-benzenediboronic acid (BDBA) and 2,3,6,7,10,11-hexahydroxytriphenylene (HHTP) were used to prepare a boronate ester-linked network as 2D COF-5 maintaining reversible condition. COF-5 utilizes hexagonal unit cell having porous sheets stacked with 0.34 nm interlayer spacing. These structures along with 2D COFs got compared in PyRD with simulated eclipsed as well as staggered arrangement; no single-crystal structure of 2D COF is available till now. COF-5 displays 1590 $m^2 g^{-1}$ BET surface area, 2.7 nm pore size distribution and very high thermal stability along with permanent porosity. In addition, self-condensation BDBA yields 2D COF and COF-1 along with COF-5 as the only example of staggered interlayer stacking, which allowed expansion of COF material via linking with organic unit covalently like B–O,

C–N, C–C [11m,5c,61]. Owing to diversity of organic synthesis, COFs offer limitless possible design space through incorporation of various functional groups for many applications. Monitoring of geometry, size and functionality of building unit is possible in both atomic layer structure as well as framework structure. Thus, COF has the liberty to offer a combination of the following properties unavailable in other materials.

Low Density: Light elements having high gravimetric performance for guest molecule are selectively used for construction of COFs to be used for energy storage. For instance, COF-108 has extremely low density of 0.1 g/cc compared to any crystalline solid.[16]

Stability: COFs, since they are linked via robust covalent bond, display higher stability when compared with most of the other materials. Very recently advancement in COFs structure took place through hydrogen bonding interference, weakening the polarity of ammine bond, incorporation of enol-keto tautomerism or following Michael-addition-elimination/benzoxazole strategy.[9,17] These approaches induce COFs to earn stability during hydrolysis, in variable pH range and redox environment, which are rarely available in MOFs.

Crystallinity: Being crystalline, COFs are able to offer the option for introduction of positional functional groups in a very precise and controlled way, providing structure property coordination and characterization by diffraction methods. Opto-electronic devices and catalysis require this potential structural uniformity too.

Porosity: Having periodic and uniform porosity, COFs ensure superior performance in catalytic reaction and gas separation due to full excess to pores. 2D and 3D COFs with 3000 and 5000 $m^3\ g^{-1}$ surface area are reported.

Modularity: Proper selection of building block before synthesis can successfully utilize versatile properties of COFs, thereby offering scientists the possibility of managing composition as well as architecture in porous and crystalline materials with control on density, functionality along with active site special arrangement. Incorporation of monomer with reduced symmetry, various components with viable length multiple bond forming process or metal coordination approaches enrich COFs structure with ability to control more sophistically. Based on functions and properties expected, COFs may have three structural label designs; skeleton, pore, and complimentary design of pore and skeleton.[18,19] COFs, a gift of nature in the form of a platform for molecular assembly are far away from complete exploitation.

2.2. *Designing principles of covalent organic frameworks*

The main aspect of COFs design is actually to extend the polymer backbone growth through elaboration of direction of covalent bond formation. Relatively rigid backbone of monomers with distinct geometry of distributed sites is needed in order to clear the direction of individual covalent bond. Within this framework, fabrication of COFs-based two/three dimensional (2D/3D) nanoarchitectures is getting immense attraction due to their tunable electronic and optical properties.[20–22] Therefore, extensive research has been conducted in the past mainly focusing on the use of COFs-based materials to utilize their intrinsic advantages in the termination of organic pollutants. In addition, the functionality of porosity with tunable structural properties of COFs might be further improved to boost the performances of these materials. The COFs structures have an extremely high porosity and a high surface-to-volume ratio, which makes them easy for molecules and ions to enter the frameworks and accumulate around the active sites.[9,23]

Within the context of the materials, the construction wedges of diverse structure and chemical properties might be systematically and logically integrated to provide synergistic function characteristics for the intended applications of COFs. Moreover, COFs are able to manipulate their spatial environment in 2D or 3D space via controlling the building block's coupling, possessing high surface area, lightness, chemical stability, low density, and simplicity of functional designs compared to traditional materials.[24] The first report on COFs synthesis was published by Yaghi *et al.*, in 2005.[25] After that, a number of different COF-based material were published, by using a wide variety of organic covalent linkers, including sp^2-carbon,[26] *b*-ketonamine,[27] phenazine,[28] triazine,[29] imide,[30] azine,[31] hydrazone or boronic ester,[32] imine,[33] and boroxine.[34] Figure 2 showed the chemical structure of some organic linkers.

COFs are formed via condensation reactions between rigid monomers and symmetrical reactive groups acting as edges or apexes. The number (n) of

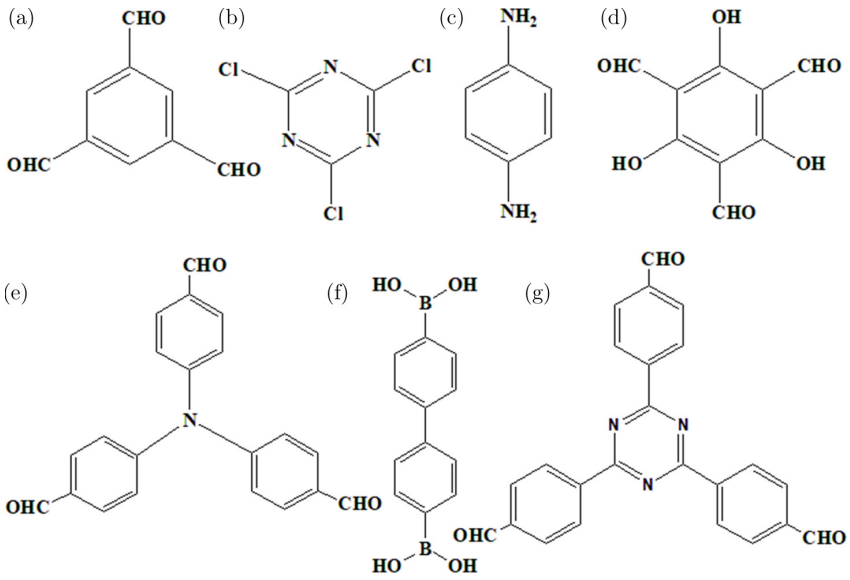

Fig. 2. Structure of (a) 1,3,5-triformylbenzene, (b) cyanuric chloride, (c) 1,4-diaminobenzene, (d) 2,4,6-triformylglucinol, (e) 1,3,5-*tris*-(4-formylphenyl)-amine, (f) biphenyl-4,4-diboric acid and (g) 1,3,5-*tris*-(4-formylphenyl)-triazine, linkers.

symmetric reactive groups in these monomers is represented by the geometry matching symbol C_n,[23] which leads to the formation of various polygon skeletons (Fig. 3). For instance, the combination of 1,3,5-tri-(4-aminophenyl)benzene (C_3) and 2,5-dimethoxyterephthalaldehyde (C_2) yields a hexagonal COF.[10] The self-adjustments of organic linkers during condensation reactions to construct the COFs architectures are partially reversible,[35] therefore, their stability as well as properties can be altered by changing the linkers.[36] significantly. Using this concept, different types of 2D/3D COFs were constructed, having good crystallinity as well as high stability. The interlayer interaction and the strength of covalent bonds are two crucial features that govern the structural stability of COFs.[37] Moreover, it is well known that COFs have varying pore architectures because of the creation of robust topological frameworks. Two basic forms of COFs exist in nature, distinguished by the dimensions of their constituent building components.[38] Most 2D COFs are fabricated by extending the covalent bonds between linker moieties to 2D atomic layers via pi–pi stacking to create highly layered structures with a high specific surface area. On the other hand, 3D COFs can be constructed using the assembly of molecular linkers or covalent linkages with a higher surface area than 2D COFs, however, due to the limited variety of tetrahedron-type knots, they are less prevalent. Out of the various synthetic approaches tried for the production of COFs, the solvothermal,[25] iono-thermal,[40] and mechano-chemical,[41] microwave-heating[42] methods were observed to be efficient and are discussed in the next sub-section in detail.

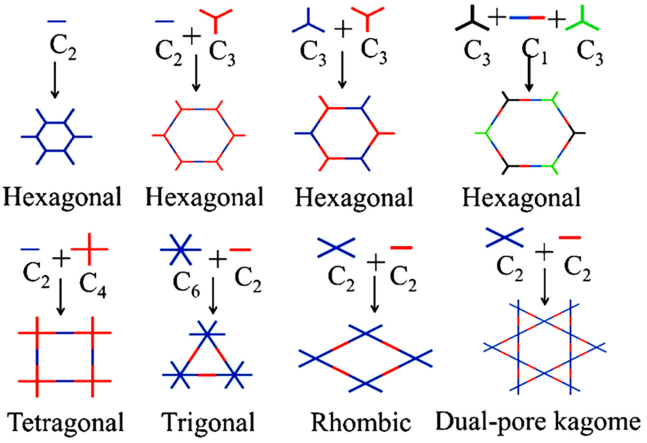

Fig. 3. Topological pictures of 2D-COFs. Taken with permission.[39] Copyrights 2019, Elsevier publishing group.

2.3. *Synthesis approaches of covalent organic frameworks*

The synthesis of organic molecules follows the protocol for irreversible bond formation monitored by kinetics. In case of reversible condition, the mismatched covalent bond gets corrected through rupture followed by thermodynamically monitored product formation, having self-healing structure.

Defect-free final structure formation from reaction components having multiple reaction sites proceeds with self-healing properties. In poly-condensation systems thermodynamically stable polymers may be produced due to reversible reaction.[43] Ordered and pre-designed connection of organic units to be linked covalently is the main theme of the topology diagram for COFs along with multiple reactive sites to support growing extended polymer structure. Reversible covalent bond formation reaction is needed for COFs synthesis.[44,45] Compound possessing phenazine linkage, dioxin linkage and C=C linkage following irreversible nucleophilic aromatic substitution reaction.[46,47] was reported to initiate the development of COFs.

Solvothermal synthesis: Solvothermal synthesis is the most widely employed protocol for COFs synthesis, in which reaction criteria depend on solubility and reactivity of building blocks along with reversibility of the reaction. In addition, to prepare crystalline porous COFs following the solvothermal process, temperature, reaction time, solvent condition, and catalyst quantity play a vital role. A synthesis strategy involves use of monomer for vertices and edges along with the catalyst and solvent being placed in a pyrex tube. The material is allowed for sonication for a short time followed by degassing through freeze-pump-thaw cycles sealed with a gas burner and rest for some time at the required temperature. The precipitate is received through centrifugation/filtration after cooling at room temperature followed by solvent washing or by soxhelt extraction. The residue gets dried at 80–120°C in vacuum and is kept under N_2/Ar in the dark. TPT-COF-1 can be synthesized using 2,4,6-*tris*-(4-aminophenoxy)-1,3,5-triazine (TPT-NH-2) on gram scale and was found to possess BET surface area of 1589 $m^2\,g^{-1}$ with high crystallinity.[48]

Microwave synthesis: Having the disadvantage of long reaction time in solvothermal strategy, microwave protocol has been tried for fast synthesis of porous COFs. Boronate-ester-linked COF-5, COF-102,[49] and imine-linked TpPa-COF.[50] are reported to be prepared successfully using microwave method. A simple microwave strategy involves sealing of a mixture of monomer solvent in microwave tube under vacuum or N_2 followed by stirring in heated condition at desired temperature for 1 h. For boron-based COF-5 and COF-102, the crude material is mixed with acetone at 65°C and stirred for 20 min. The precipitate is collected via filtration and dried in vacuum. The important feature of microwave solvent extraction method is that it can discard oligomers easily and COFs have better porosity.

Iono-thermal Synthesis: In spite of the fact that they possess a variety of monomers, the majority of the CTFs are amorphous and are short of large molecular orderings. However, CTF-1 and CTF-2 prepared in iono-thermal conditions possess crystalline porous materials.[45] Typically, $ZnCl_2$ along with monomer is kept in Pyrex ampule, sealed, and followed by heating at 400°C for 40 h. Following heating, it is cooled, crushed and washed with water to remove excess $ZnCl_2$. The powder in dilute HCl gets stirred for 15 h to remove any $ZnCl_2$ left, filtered followed by washing with H_2O and THF and dried in vacuum to obtain CTF-1 and CTF-2. Molten salt, during synthesis, acts as solvent along with catalyzing the trimerization reaction simultaneously, which is believed to be reversible at this temperature. CTF-1 synthesis using para-toluene sulfonic acid as catalyst in microwave condition has been reported recently.[51] In this context, ionic liquid if used as solvent may offer green and simple synthetic protocol to prepare 3D COFs and a series of many 3D COFs ionic liquid possessing COFs have been reported.[52]

Mechanochemical Synthesis: It is well known that both solvothermal and microwave methods are employed with lots of complications which prompted researchers to search for a reliable and simple synthetic protocol for this purpose. Mechanochemical synthesis proceeds through bond formation via cost-effective, ecofriendly simple route addressing the limitations of solvothermal methods. In this approach, monomers are grounded in mortar at room temperature to prepare COFs including TpPa-1, TpPa-2, TpPa-NO_2, TpPa-F4, TpBD, TpBD-$(NO_2)_2$, TpBD-Me_2, and TpBD-$(Ome)_2$.[52,53] In order to utilize the entire potential of this protocol in properly optimized mechanochemical conditions, the grinding method assisted by liquid is already developed. A little quantity of catalyst is mixed in the mortar in order to increase the reaction rate via facilitation of uniformity of reactants, which eventually brings better crystallinity.

2.4. *Modification in covalent organic frameworks-based architectures*

Changing the architectures on which COFs are based is an intriguing way to take advantage of their chemical features. Changing the linkers or chemically altering the structure of the organic linker are common approaches to manipulate the COFs. Besides, the coordination allows a single metal atom to bind to numerous ligands, which increases the strength of the immobilization and the stability of the system.

The OH-containing imine-linked COF[55] demonstrated that a chelating Schiff base could form a robust coordination bond with metals. It has also been shown that these COFs are thermally stable at temperatures above 350°C. Finally, ligand sites for metal attachment can be made by using the ligand activity already present in the monomers.[56,57] The most extensively utilized linkers in the production of COFs possessing ligand functionality are porphyrins in particular. These organic compounds are extensively studied as biomimetic catalysts. The porphyrin ring's core pyrrolic N-donor atoms can stabilize most of the metal ions.[54,58] Figure 4 depicts a scheme of metalized porphyrin COFs.

Furthermore, COF tunability is a measure of their applicability[60,61] To functionalize COFs, addition and substitution operations are the most common approaches. After synthesis, COFs can be altered by incorporating more functional groups to increase their usefulness in various applications. Therefore, aromatic and aliphatic moieties containing –COOR, –COOH, –OH, and –SH functional groups can be incorporated into the COF frameworks via chemical reactions[62,63] (Fig. 5). Alkyl chain halogenation,[64] alkali metal salt production,[65] and aromatic nucleophilic substitution of aryl fluorides[66] are also other ways to change the structure of a molecule. Usually, prepared COFs occur in the form of polycrystalline solids which normally exhibit crystalline-type domains with average range of ∼ 50–500 nm,[67] indicating bulk COF particles (100–1000 m) being formed by aggregation of NPs crystallites (Fig. 6).

Synthetic approaches are commonly employed to control crystallite size and development through multi-dimensional covalent polymerization.[69] The amorphous phase gets suppressed by thermodynamic and kinetic monitoring, allowing the crystalline phase to grow.[70,71] Multiple nucleating sites, on the other hand, stifle development and cause crystallization defects, resulting nanoscale crystalline growth of most COFs. The assembling of

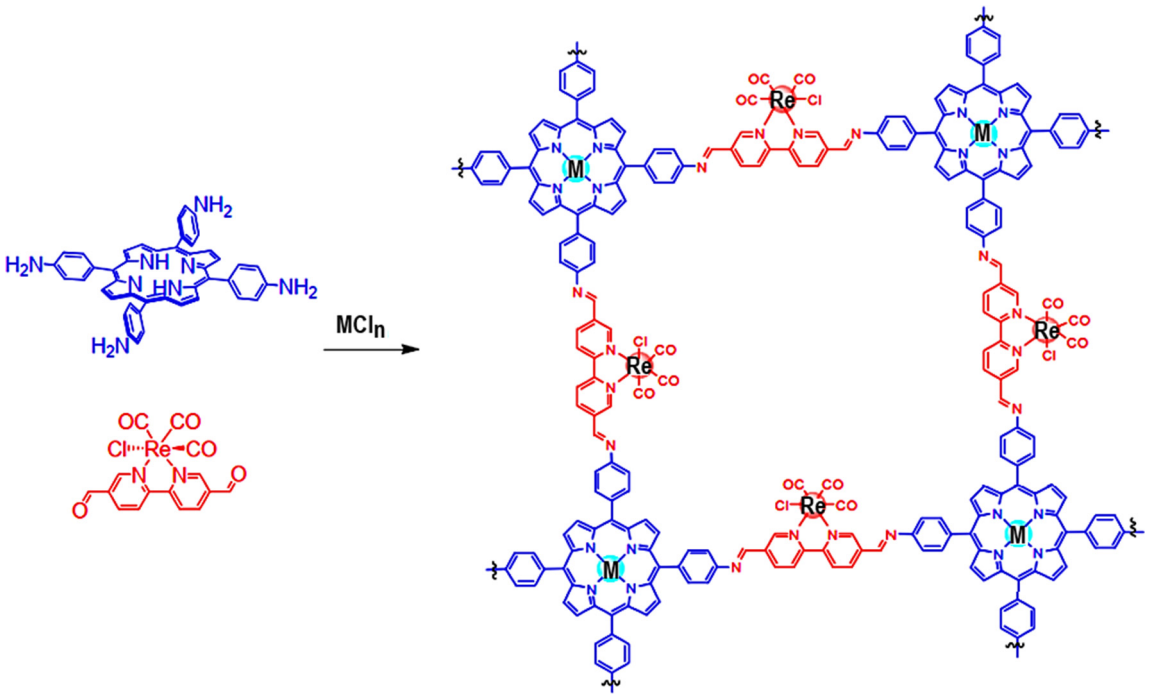

Fig. 4. Assembly of pre-metalized/post-metalized Por-based COFs. Taken with permission.[54] Copyrights 2018, ACS publishing group.

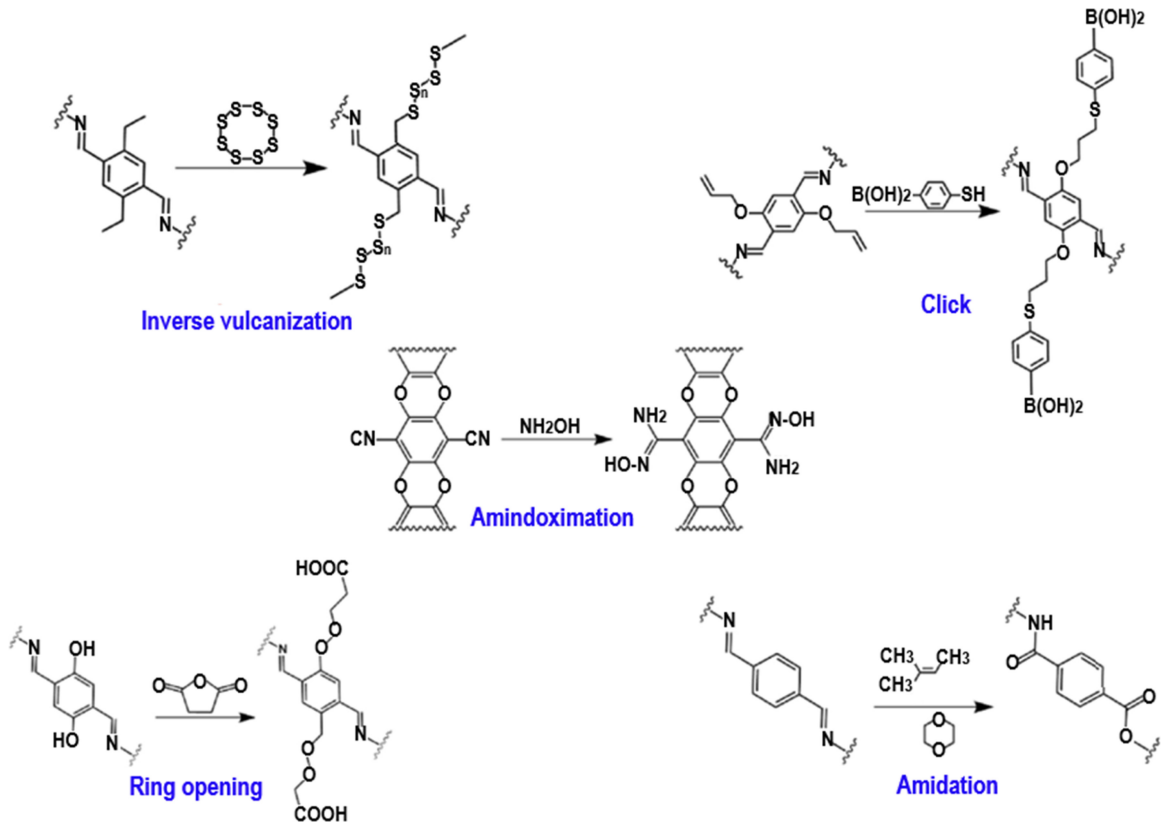

Fig. 5. Illustration for the COF's functionalization. Taken with permission.[59] Copyrights 2021, Elsevier publishing group.

multiple crystallites into many nanostructures determines the ultimate bulk COF state. The aggregation of assembly of these nanosized motifs created at the time of synthesis provides guideline for bulk solid construction. Crystalline growth usually creates three main nano-sized motifs: (i) nanosheets, (ii) nanofibers, and (iii) nanospheres.[72,73] When growth happens along one dimension (x or y), nanofibers are formed, while nanosheets are formed when growth occurs along both dimensions (x and y). Nanospheres are formed via the confinement and peripheral stability of edge-crystallites. Such nanostructures are made using dynamic polymerization, and they commonly crystallize outside of the reaction system. As a result, these nanostructures may be segregated with the limitation of lack of justification for the same. Belts, cubes, rectangular prisms, platelets, and other known COF nano-morphologies (e.g., belts, cubes, rectangular prisms, platelets, and so on) are framework-specific and thus outside the scope of this review.[74,75] Table 1 shows the synthesis strategies and properties of the COF-based materials.

3. Applications of COFs-Based Materials for the Taming of Organic Pollutants

3.1. *Photodegradation organic pollutants*

Due to their high light absorption and narrow bandwidth, COFs show significant promise as semiconductor photocatalytic materials. These characteristics make COF a promising contender as novel heterogeneous photocatalysts, and some obstacles must be overcome before they can be used in environmental cleanup. COFs have fast photocatalytic activity because photo-electron–hole pairs move slowly and the first recombination happens quickly. Several reports are available on high-performance ligands for designing high-performing photocatalysts to degrade organic pollutants.

When exposed to light, the COF undergoes electronic transitions that produce photogenerated carriers like electrons and holes. Standard operating procedures for photocatalytic degradation methods of various COF composite materials typically adhere to the aforementioned conditions. Due to

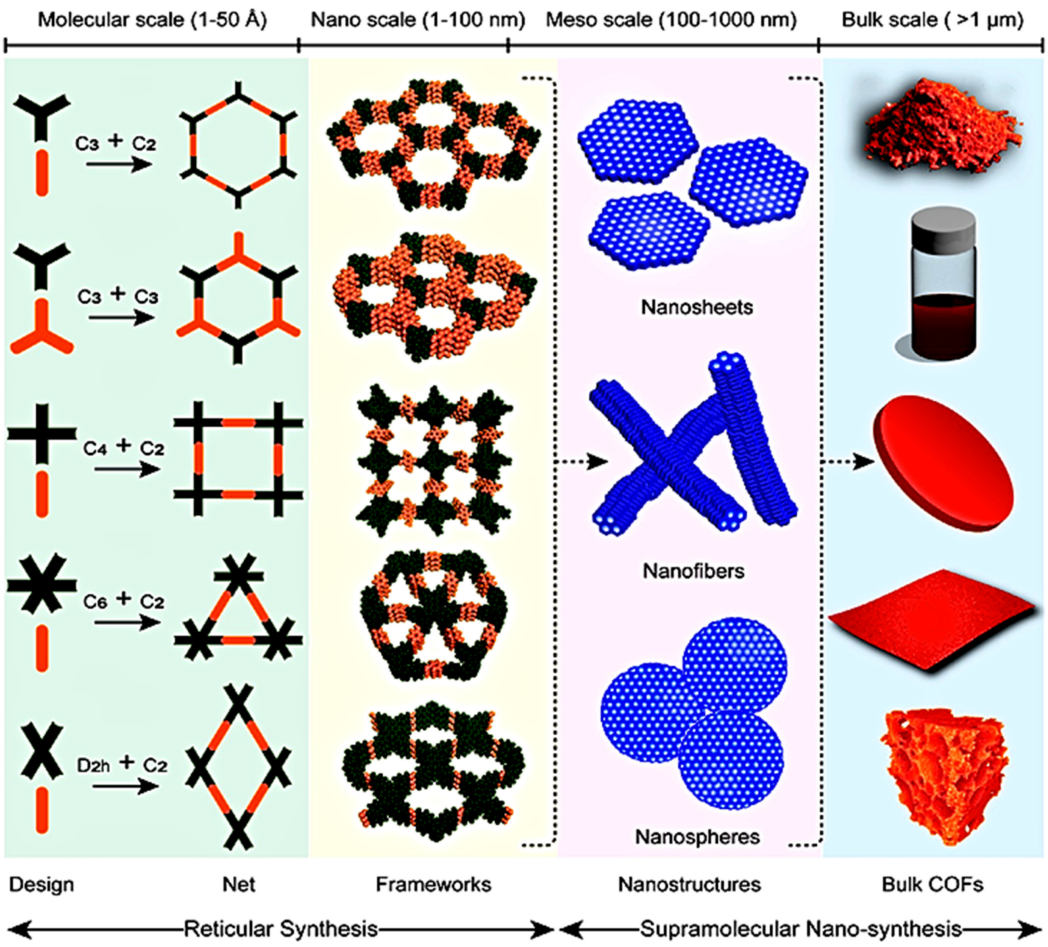

Fig. 6. A systematic transformation of molecular systems into bulk components by means of COFs materials. Taken with permission.[68] Copyright 2012, ACS publishing group.

their unique properties, COF materials and composite materials have different valence and conduction band configurations. Unfortunately, it is currently unable to generalize the photocatalytic process of many COF-composites. The photocatalytic process is known to work by taking in light, separating electron–hole pairs, and moving electrons. Photocatalysts can be judged by their electronic states and their ability to absorb light by looking at their diffuse reflectance spectra in the ultraviolet–Vis range. Photocurrent

Table 1. Synthesis strategies, and properties of COF-based materials.

COFs	Synthesis method	Critical parameters	BET surface (m^2/g)	Pore volume (cm^3/g)	Pore size	Crystal structure	References
PS-COF-1	Solvothermal	80°, 72 h	2703	2.68	~ 4.5 nm	2D layered crystal	76
o-GS-COF	Solvothermal	120°, 12 h	51.5				77
COF-HAP	Solvothermal	120°, 72 h	26.9	0.14	15 Å	Crystalline	78
TaTp-1COF/CDs	Hydrothermal	Room temperature	76		2.59 nm	Core–shell, 2D layered crystal	79
COF@PDA	High-temperature condensation polymerization	180°, 72 h	118.2			Core–shell structure, amorphous	80
Fe_3O_4@COFs	*In situ* growth	Room temperature	55.7	0.12		Core–shell structure	81

responses and electrochemical impedance spectroscopy (EIS) are studied to assess more about MOFs' charge-separation performance. A PL emission spectrum can be used to verify the charge transfer procedure. Since PL signals are produced by the recombination of photogenerated electron–hole pairs, they can be used to analyze the entrapment, migration, and transfer of photogenerated charge carriers (Fig. 7).[75]

Within this framework, Jiang *et al.*,[83] used different metal core porphyrins to make a set of new 2D COFs. In this study, MP-COFs were broken down into their parts, which were a core porphyrin monomer and different metals, to find out how their carriers moved through them. Material made from zinc porphyrins (ZnP-COF) and material made from copper porphyrins (CuP-COF) had the same hole and electron conduction properties (Fig. 8). Porphyrin COFs provide two distinct paths for electrical current to flow: hole conduction through adjacent porphyrin molecular layers and electron conduction through porphyrin metal cores. In MP-COFs' multilayer stack architectures, adjacent core metals play a significant role in creating conductive channels and regulating carrier movement. Because

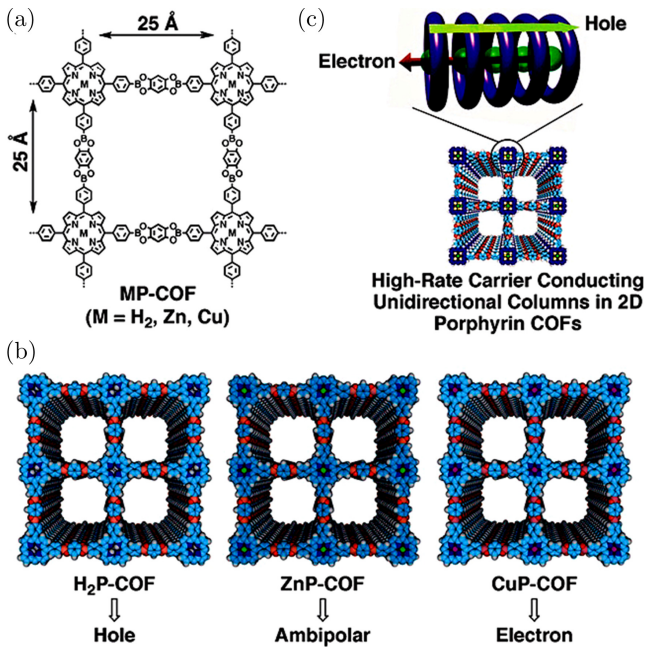

Fig. 8. (a) Crystallographic illustration and (b) a 2×2 grid 2D sheet of MP-COFs. (c) Representation of (e) transfer mechanism 2D porphyrin COFs. Taken with permission.[83] Copyright 2012, VCH welly publishing group.

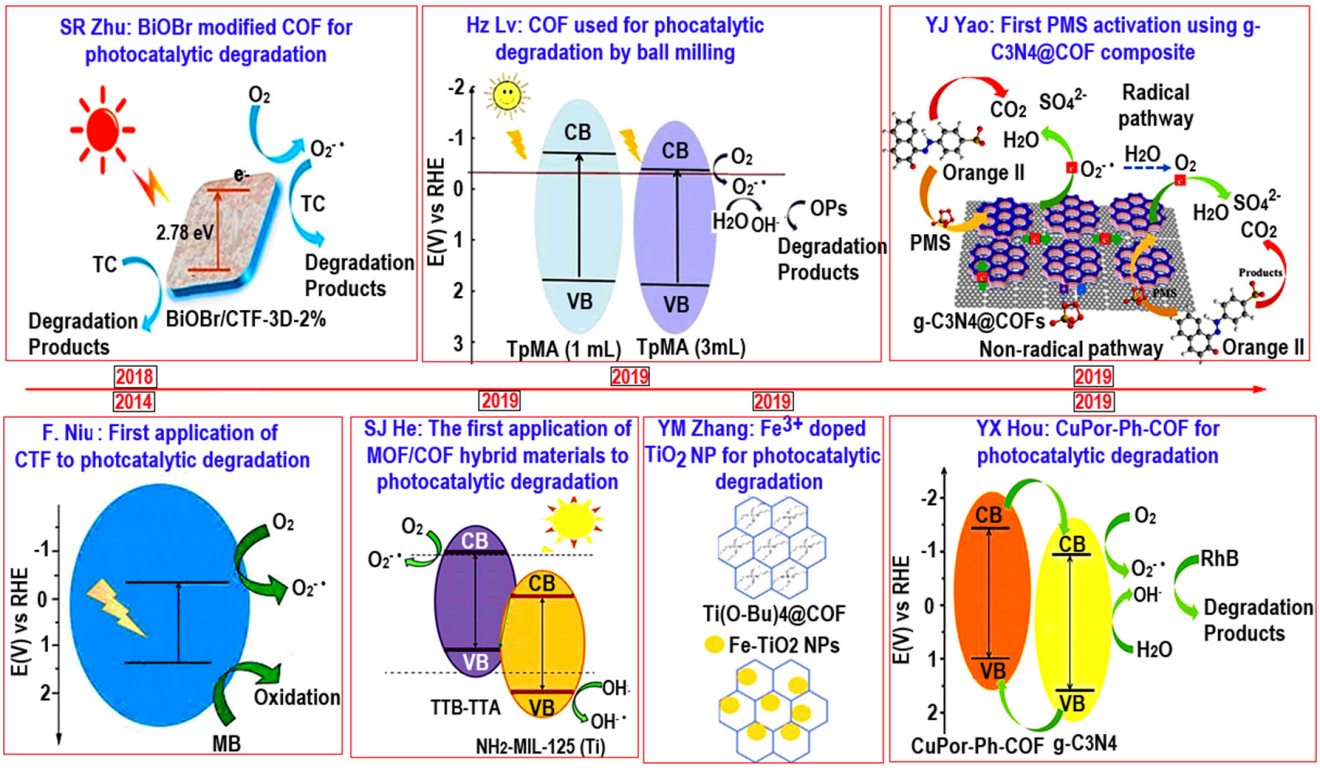

Fig. 7. Roadmap of COFs progress towards photocatalytic degradation. Taken with permission.[82] Copyrights 2022, Elsevier publishing group.

porphyrin metal centers can be used in different ways, they have future prospects in the field of catalysis.

Moreover, the Cu-porphyrin-based COFs, as efficient photocatalysts for the breakdown of organic pollutants, are emerging materials for environmental remediation. Studies of iron porphyrin-based COF photocatalysts for the breakdown of organic pollutant compounds are still in their infancy.[84] For instance, conducting the Sonogashira–Hagihara coupling reaction between iron (III) 5,10,15,20-*tetrakis*-(4-bromophenyl) porphins and 1,4-diethynylbenzene was utilized to construct the Fe-porphyrin-based COFs and applied for the photocatalytic degradation of organic pollutants. The prepared material has shown good dye degradation under visible light irradiation, demonstrating satisfactory performance for the degradation of organic polluting substances photocatalytically. This research work paves the way for the potential applications of porphyrin iron carbonate oxalate-based COF in photocatalytic degradation.

It has become a common practice to use photocatalysts to convert peroxymonosulfate (PMS) or peroxydisulfate (PS) to SO_4• for wastewater treatment. Since SO_4• has a high oxidizing potential and may efficiently degrade new contaminants, it is preferable to •OH. Two novel MOFs@COFs hybrids were originally synthesized by Lv *et al.*[85] using post-synthesis methods; these hybrids include Nrch structural units that activate PS to create SO_4•, resulting in the breakdown of bisphenol A. In conclusion, the solvothermal method was used to generate MOF materials like MIL-101-NH_2 and UiO-66-NH_2, as well as TpMA-based COFs. In addition, two other MOFs@COFs hybrids, MIL-101-NH_2@TpMA and UiO-66-NH_2@TpMA, were also prepared via covalent linkages between MOFs to COFs under solvothermal methods [Fig. 9(a)].

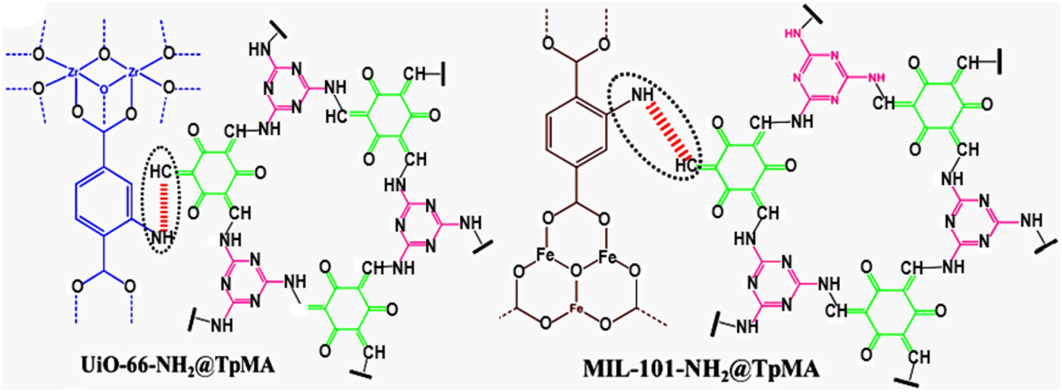

(a)

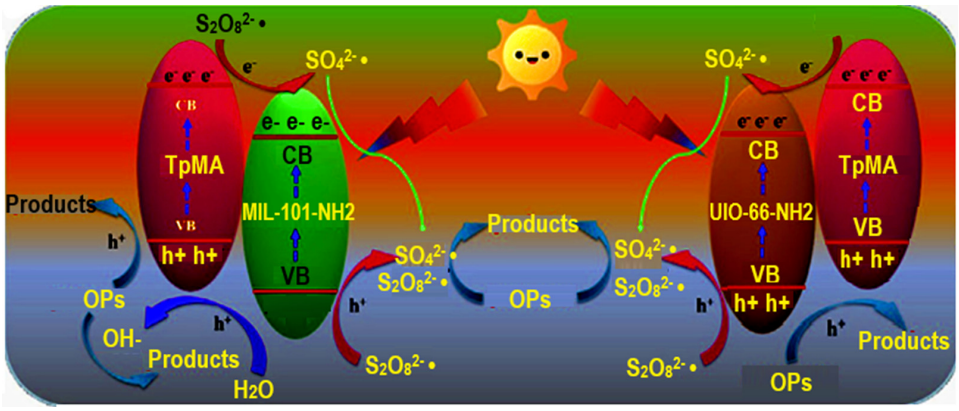

(b)

Fig. 9. (a) Chemical structures of UiO-66-NH_2@TpMA and MIL-101-NH_2@TpMA and (b) proposed photocatalytic mechanism towards BPA degradation for MIL-101-NH_2, UiO-66-NH_2, COF-TpMA, MIL-101-NH_2@TpMA and UiO-66-NH_2@TpMA. Taken with permission.[85] Copyrights 2020, Elsevier publishing group.

These MOFs@COFs-based hybrids were shown to have potential to degrade BPA. Degradation efficiency is influenced by three primary factors: (i) the strong oxidizing capacity of $SO_4^{\bullet}$, (ii) the development of heterostructures, and (iii) an increase in the specific surface area of hybrid materials. Therefore, the incorporation of PS drastically increased BPA breakdown efficiency, revealing the critical function of $SO_4^{\bullet}$ in BPA oxidation. Moreover, the process depicted in Fig. 9(b) was proposed as an explanation for the hypothesized photocatalytic effect. In this approach, $SO_4^{\bullet}$ played a major role in the decomposition of organic contaminants, and the process by which these structures got formed was referred as hetero-structure formation. The fact that the PL strength of the composites MIL-101-NH_2@TpMA and UiO-66-NH_2@TpMA was lower than the parent materials demonstrates that electron-recombination of the hole pairs was effectively suppressed.

This change was motivated by three factors: (ii) an increase in hybrid material specific surface area; (iii) the ability of heterojunctions formed at the interface of MIL-101-NH_2, (or UiO-66-NH_2) and TpMA to further separate photogenerated electron–hole pairs. Specific surface area was calculated using N_2 adsorption–desorption isotherms, revealing a range of increases among materials. Increases in specific surface area result in a greater number of potential active sites, which can boost photocatalytic efficiency. On the other hand, during photocatalytic degradation, the role of free radicals is widely acknowledged. Nonradical processes of certain materials, such as singlet oxygen and direct electron transfer, have also been observed and reported with free radicals (SO_4• and •O_2)[86] In this work, the authors demonstrate the photocatalytic degradation of Orange II under PMS-mediated AOP conditions by anchoring COF to the surface of g-C_3N_4 using a post-synthesis modification approach, resulting in a unique metal-free 3D-structured catalyst. Figures 10(a) and 10(b) depict the composite synthesis of COF (mechanical grinding method), g-C_3N_4, and g-C_3N_4@COF. To create g-C_3N_4, its three precursors (urea, melamine, and dicyandiamide) were cooked in a muffle furnace at 550°C for 4 h. Different g-C_3N_4@COF composite materials were developed following the discovery of their porous structure and properties. Using urea as a precursor, UCN@COF's activity was observed to be the most productive. The unique synthesis between UCN and COF led to a high N concentration of 25.2% in the UCN@COF, which was superior to most of the reported N-doped carbon materials.

In addition, using nanocarbons as support for the catalyst, hetero-atoms-doping the COFs-architecture, electronic conductivity may be significantly improved if electron-deficient N species were responsible for easily breaking the sp^2-hybridized carbon's chemical inertness and boosting the positive charge density on neighboring C atoms. Interestingly, the opposite conclusion to the commonly held mechanism for PMS activation was reached. Both EPR and quenching tests showed that oxygen (O_2), and not hydroxyl or sulphate, was the primary reactive species in the g-C_3N_4@COF/PMS system. It was generally accepted that PMS might spontaneously combust into oxygen.

For instance, in the case of UCN@COF, PMS generated an unstable intermediate with the sp^2-hybridized carbon networks, and the highly covalent p electrons may have triggered the PMS O–O bond to interact with adsorbed organic moieties in a nonradical fashion. Additionally, it is possible that •O_2 is the primary reason for efficient $^1O_2$ generation in the UCN@COF/PMS system. Here, BQ was employed to quench the production of oxygen (O2). Orange II's degradation was halted by BQ, suggesting that •O_2 was created in this system. As a catalyst, UCN@COF has the potential to increase PMS hydrolysis, leading to more production of O_2. The oxidative treatment of organics by UCN@-COF/nonradical PMS was successful because UCN@COF facilitated the passage of electrons from Orange II to PMS. Within 45 min of implementing the UCN@COF/PMS system, Orange II had entirely degraded. The high specific surface area, rapid mass transport, additional N-active sites, and synergistic action of g-C_3N_4 with COFs to create O_2 are all responsible for the remarkable activity of the resulting UCN@COF.

Several types of semiconductor metallic photocatalysis have been described during the past two decades to convert organic polluting substances into biodegradable molecules, including TiO_2, ZnO, CdS, and others. On the other hand, these photocatalysts have a number of drawbacks, including a high band gap and photo-electron–hole combination, which reduces catalytic efficiency. Furthermore, under normal operating conditions, such catalysts are unstable. Corrosion is commonly

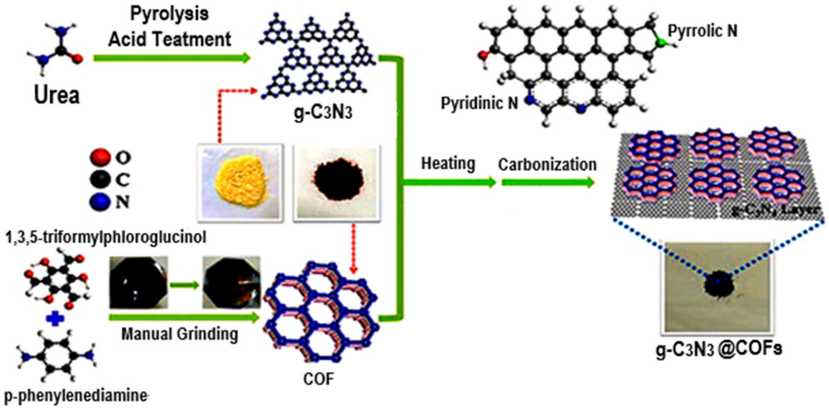

(a)

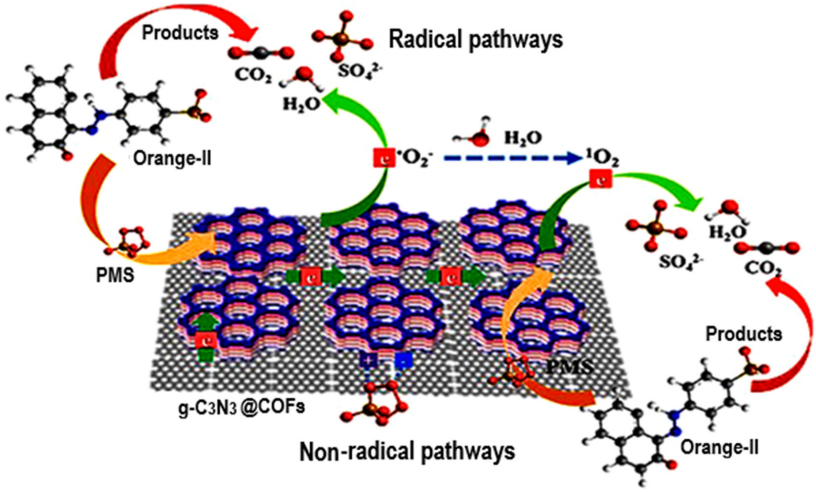

(b)

Fig. 10. (a) Fabrication process for g-C_3N_4@COF and (b) proposed radical/nonradical reaction pathways towards catalytic oxidation of organic pollutants. Taken with permission.[86] Copyrights 2019, Elsevier publishing group.

caused by irradiation in water-based systems. The COFs with inorganic semiconductor photocatalysts are seen as a promising approach to address these issues. For the degradation of bisphenol A, Sun *et al.*[87] synthesized a CdS/COF composite photocatalyst using an ultrasonic-assisted synthesis method (BPA). Figure 11 illustrates the preparation of CdS/COF composite, which has the highest photocatalytic activity for BPA degradation, degrading 85.68% of BPA in under 3 h with 0.3 g/L as optimum CdS/COF dose for BPA breakdown. BPA degrades differently depending on the pH of the surrounding environment. At a pH of 10, BPA was easily adsorbed onto the catalyst surface, having the greatest possible degrading effect. Together, h^+, •OH, and $•O_2$ will degrade BPA, with h^+ and $•O_2$ playing crucial roles. Studies on cycling showed that 0.5 wt.% CdS/COF was stable and reusable for BPA degradation.

3.2. *Adsorption of organic contaminants*

Because of their ability to alter the oxygen/nitrogen balance of water, COFs pose a threat to aquatic life and eco-systems. They can spread pollution over a wide region through rivers and streams. In many circumstances, only a tiny amount of the toxin is needed to cause serious problems for eco-systems and human health. Therefore, before being released into a water system, organic contaminants should be cleaned up as thoroughly as feasible. Therefore, organic pollutants must be eliminated as much as possible prior to being discharged into a water

system.[88,89] Broadly resilient, and stable porosity, as well as appropriate surface functional groups, have shown promise for the adsorption of bulky chemical compounds in COFs. Different adsorption methods are available depending on the pollutants and the COF used. Key adsorption mechanisms include the pore-size effect,[89] H-bonding,[90] hydrophobic interaction,[91,92] and *p–p* interaction,[91,92] as illustrated in Fig. 12 .

The capture of arylorganophosphorus flame retardants[89,93] reveals that the pore size itself may be the deciding factor in the removal of a certain adsorbent. It has been observed that pharmaceutical chemicals can be adsorbed to materials based on COF. As shown by Akpe *et al.*,[93] triazine COFs had a sulfamethoxazole antibiotic removal capability of 483 mg/g in water. Primarily, adsorption occurred through contact and hydrophobic interactions. Selective adsorption employing two different COFs with NO_2 (COF-NO_2) and $–NH_2$ (COF-NH_2) functionalities has been described for the NSAIDs ketoprofen, ibuprofen, and naproxen.[94] In this case, the adsorbent's pore size was found to be responsible for TS-high COF-1's adsorption capacity for MB (1691 mg/g). The high adsorption capacity of TS-COF-1 for MB (1691 mg/g) was attributed to the small pore size of the adsorbent and the large size of the adsorbate.[95] Researchers have also looked at the possibility of employing *b*-cyclodextrin (b-CD)-based 3D crystalline

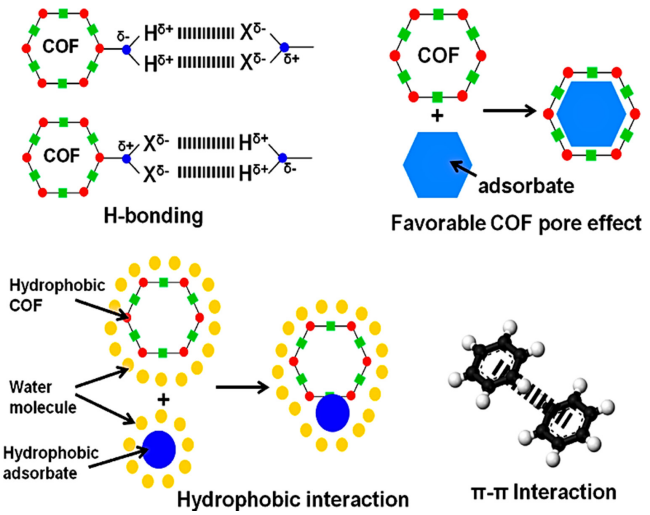

Fig. 12. The interaction communication between adsorbate and COF. Taken with permission.[97] Copyrights 2021, Elsevier publishing group.

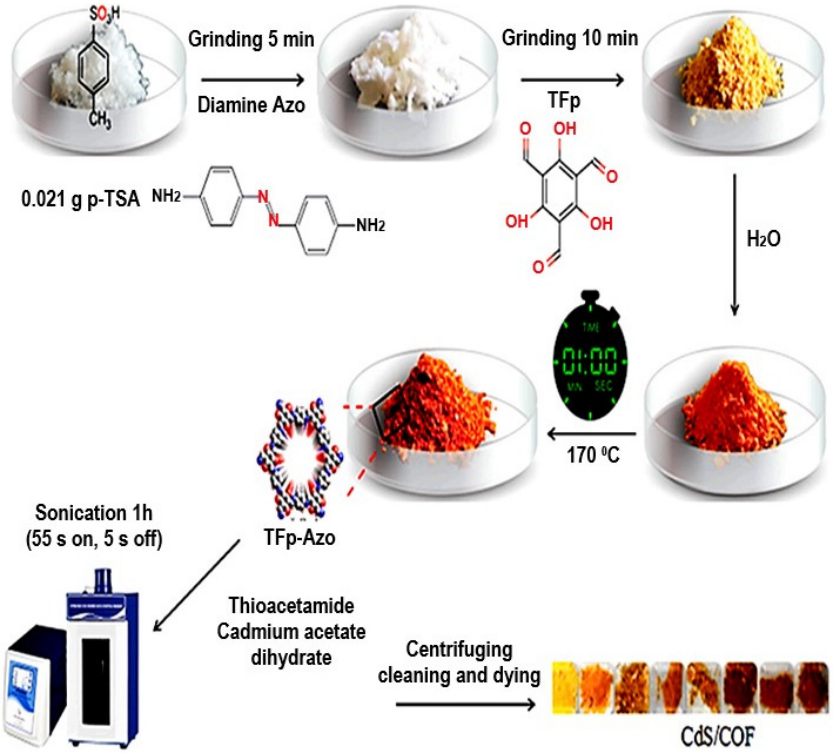

Fig. 11. Protocol for the preparation of hetero-structured CdS/COF hybrid. Taken with permission.[87] Copyright 2021, Elsevier publishing group.

COFs for the adsorption and removal of polar micropollutants.[96]

3.3. *Dye removal, (organic pollutant removal) from the water sample*

Most COFs include inherent holes with diameters between 1 and 3 nm, making them optimal for dye separation. There are two ways to get rid of dyes made with COF. Most often, NF is used to get rid of dyes by means of a membrane. COFs can be made by injecting COFs into a membrane matrix, or they can be made directly from COFs. In this case, pore size plays a major role in dye removal. The second method is a charge- and size-selective process known as dye molecule adsorption on COFs particles.

COFs have been used in membrane technology for dye removal in a variety of methods. Interfacial synthesis is a common approach for creating the COF membrane. Dey *et al.* reported four kinds of interracially crystallized COF (Tp-Bpy, Tp-Azo, Tp-Ttba, and Tp-Tta) free-standing thin films.[98] Among these COFs, Tp-Bpy COFs [Fig. 13(a)] displayed dye rejection values as high as 94%, 80%, 97%, and 98% toward blue-G, congo red, acid fuchsin, and rhodamine B, respectively. Water permeance was measured to be as high as 211 L m^{-2} h^{-1} bar^{-1}. Zhang *et al.* employed interfacial crystallization to make EB-COF:Br nanosheets, which are a 2D cationic COF. Because of the abundance of positive charge sites in its pore walls, the EB-COF:Br membrane was able to reject over 98% of anionic dyes (methyl orange, fluorescein sodium salt, and potassium permanganate) while maintaining a high water permeance (546 L m^{-2} h^{-1} bar^{-1}).[99] Wang's group published a work using Tp and Pa interfacial polymerization to grow imine-type COFs directly on PSf substrates to build composite membranes. The membrane demonstrated a stable Congo red dye rejection of 99.5% and a low water permeance of 50 L m^{-2} h^{-1} bar^{-1} when it was constructed.[100]

Banerjee's group demonstrated self-standing and crystalline COF membranes using a simple process

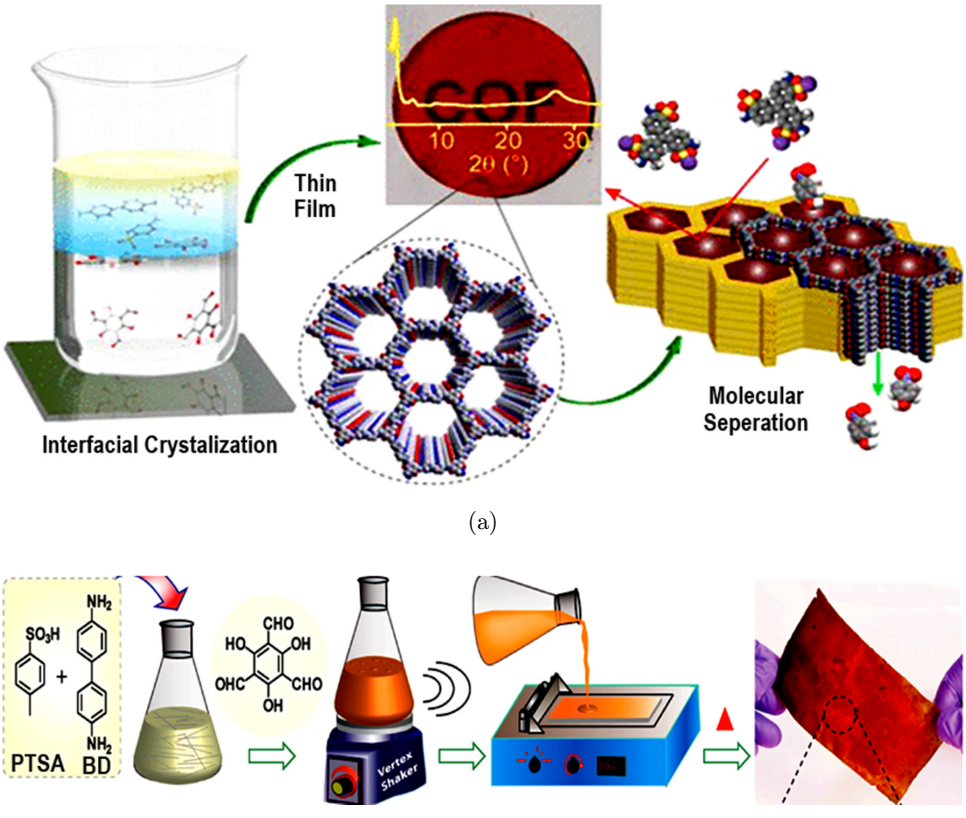

Fig. 13. (a) Graphical representation of the interfacial crystallized COF-Tp-Bpy for the selective separation of dyes[98] and (b) free-standing COF-Tp-BD. Taken with permission.[114] Copyrights 2017, VCH welly publishing group.

of baking the molecular precursor [Fig. 13(b)].[101] The as-synthesized M-TpBD COF membranes could reject rose Bengal to the tune of 99%, while 96% and 94% reflections under water performance of around 120 L m^{-2} h^{-1} bar^{-1} were observed in Congo red and methylene blue, respectively. To prepare COF membrane free from defect, Pan *et al.* demonstrated a modification of polyacrylonitrile (PAN) porous substrate surface with –CHO groups as nucleation sites, followed by depositing a continuous imine-based COF layer [TpPa-1, synthesized by Schiff-base reactions of 1,3,5-triformylphloroglucinol (Tp) with *p*-phenylenediamine (Pa-1)].[102] Orange GII was rejected 94% of the time by the TpPa-1/HPAN membrane, while Methyl blue, Congo red, and Alcian blue were rejected over 99%. The TpPa-1/HPAN membrane rejected Orange GII 94% of the time, while Methyl blue, Congo red, and Alcian blue were rejected over 99%. Fan *et al.* used an *in situ* solvothermal method to fabricate continuous 2D imine-linked COF-LZU1 membranes, having 400 nm thickness on alumina tubes. It displayed a water permeance of 760 L m^{-2} h^{-1} bar^{-1} MPa and a rejection rate of 90% for dyes more than 1.2 nm. Table 2 shows the OPs taming performance of various COF-based materials.

Chemically and thermally, these membranes were likewise stable.[110] COF-1 crystals were inserted into GO membrane surfaces using an *in situ* growth method developed by Zhang's lab.[111] Excellent dye rejection (> 99% for Congo red, Methylene blue, Reactive Black 5, and Direct red) was achieved using a combination of COF-1's physical size sieving and an optimum interlayer spacing between the GO sheets. Sun's team used vacuum filtering and hot pressing to insert COF-TpPa onto GO membranes for dye removal in the same year.[112]

The fabricated membrane, HP-COF-TpPa/GO, revealed significantly improved stability under universal pH conditions, with a water permeance of 166.8 L m^{-2} h^{-1} bar^{-1} and an effective dye rejection rate of 97.05% for methylene blue. Ning *et al.*,[113] developed a salicylideneaniline-based chemo-selective COF (SA-COF) that underwent tautomer exchange in response to a solvent. When tautomerization is used to modify the COF's ionic properties, the resulting SA-COF has a pore surface functionality that may be tailored for size-, charge-, and functionality-based molecular separation.

3.4. *Taming of organic pollutants via other materials*

Although COF-based materials have been considered promising materials for OP taming, as discussed earlier. Apart from the COF-based materials, other materials like MOFs and carbon-based materials are also acknowledged for OP taming.[115] On the other hand, metal-organic frameworks (MOFs) are a suitable substrate to control OPs due to their malleable pore topologies, high surface areas, and thermal and chemical stability.[115] The key mechanisms by which OPs interacted with MOF-based materials were H-bonding, electrostatic attention, pi–pi interaction, and surface complexation. The binding of OPs was influenced by porous architectures, inner pore sizes, and surface groups.[116] Besides, the carbon-based materials, including activated carbon, black carbon, carbon nanotubes (CNTs), graphene oxide (GO), etc., have

Table 2. The adsorption performance of COF-based materials towards various Ops.

Materials	Target	Adsorption equilibration time (min)	Adsorption capacity (mg/g)	Adsorption mechanism	References
TpBD-Me 2-COF	Okadaic acid	60 min	279.0	Heterogeneous adsorption	103
COFs	2-Nitrophenol	90 min	239.9	*p–p* interaction; different size values; surface complexation	104
COF-3	TPhP	12 h	371.2	Hydrogen bonding; *p–p* interaction; different size values	105
TPT-DMBD-COF	MB	60 min	45.5	Electrostatic attraction; *p–p* interaction	106
TPT-TAPB-COF	RhB	90 min	970.0	Homogeneous adsorption	107
CuP-DMNDA-COF/Fe	RhB		378.0	Surface complexation	108
Magnetic TPB-DMTP-COF	Diclofenac	50 min	109.0	C–H interaction; *p–p* interaction	109

Table 3. Comparison between the performance of COFs, MOFs, and carbon materials towards OPs taming.

Materials	Target	Adsorption capacity (mg/g)	Adsorption mechanism	References
COF TpPa-1	BPA	1424.27	Hydrogen bonding and π–π inter action, occupied in the pore cages	120
COF/GO	RhB	368	Electrostatic interaction, H-bond, π–π interaction	121
COF/GO	MB	328	Electrostatic interaction, H-bond, π–π interaction	122
CuP-DMNDA-COF/Fe	RhB	378.0	surface complexation	108
Magnetic TPB-DMTP-COF	Diclofenac	109.0	C–H interaction; *p*–*p* interaction	109
MOF-MFC-N	MB	128	Electrostatic and *p*–*p* stacking interaction	123
MOF MFC-O	MO	219	Electrostatic and $p-p$ stacking interaction	123
Active carbon	Phenol	257	Electrostatic interaction, H-bond, π–π interaction	124
Active carbon	2,4-Dichlorophenol	232.56	Electrostatic interaction, H-bond, π–π interaction	125
Active carbon	RB-2	0.27	π–π interaction	126
Active carbon	RB-4	0.24	π–π interaction	126
Active carbon	MB	180	π–π interaction	127
Mesoporous carbon CMK-3-100°C	Phenol	347	π–π interaction	125
Mesoporous carbon CMK-3-130°C	Phenol	428	π–π interaction	125

been widely utilized for OP taming.[117] Carbon materials offer the diversity in physicochemical interactions necessary to interact with OPs via electrostatic, C–H bonding, pi–pi stacking, and hydrophobic forces.[118] However, on the basis of different nanostructures, sizes, pore sizes, volume, surface area, and functionalities, carbon materials also show variation in their performance towards OP taming. Among various types of carbon materials, activated carbon materials have been widely used as adsorbents for OPs.[119] However, the adoptable strategy is a complex method with many challenges to address. The difficulty is the result of a large number of variables, including dispersive, electrostatic, and chemical interactions, along with the intrinsic properties of the solute (like solubility) and the intrinsic properties of the adsorbent. Table 3 shows a comparison between the performance of COFs, MOFs, and carbon materials towards OPs taming.

4. Conclusion and Future Prospects

Covalent organic frameworks (COFs) are constructed from the association of organic linkers through covalent interactions, resulting in a highly crystalline and porous organic 2D/3D architecture. In turn, the existing documentation of multiple fabrications and connection procedures contributes to their synthesis with several valuable qualities and their further usage in a wide range of applications. This is because they occupy a precisely determined location in 2D or 3D space, which agrees with the planned and predetermined bonding of monomer linkers. By utilizing post-synthetic modification or conversion techniques, COF-based materials with improved chemical and physical properties can be fabricated. Because of their extraordinary surface area, porosity, structural designability, low density, crystallinity, biocompatibility, and chemical stability, COFs are finding increasing use in a wide variety of fields, such as energy conversion and storage, electrocatalytic processes, photocatalysis, organo-catalysis, adsorption, separation, sensing, optoelectronic devices, and biomedicine. Focusing on the construction and state-of-the-art progress connected to the spectrum of environmental remediation, this article analyzes the numerous reactions and methods for the synthesis of 2D and 3D COFs (i.e., removal of organic pollutants). There have been substantial developments in COF-based materials for the above applications, but there are

still many challenges to be met. The following topics warrant further investigation:

(i) A synthesis approach needs to be created so that material architectures can be controlled and the structure-property relationship can be understood. It is well documented that the ability to adsorb or desorb intermediates and reactants will vary depending on the architecture used. In a catalytic reaction, the structure has a major impact on how well it works. It is essential to develop synthesis procedures to control the surface chemistry of catalysts in order to study their reaction mechanisms and make additional improvements to their performance.

(ii) Knowing how structure affects physical properties is crucial to grasping the nature of chemical processes. When the structure of a catalyst is altered, its physical properties, such as its ability to distribute and transfer electrons and ions, are affected. Incorporating physical features into the design of electrocatalysis structures is only getting started. Consequently, scientists need to zero in on the materials themselves and come up with new ideas for enhancing the reaction mechanism.

(iii) It is vital to combine academic research with the needs of manufacturing. Most current studies concentrate on improving catalysis performance by doping catalysts with heteroatoms or creating them in nanostructures. Almost no research has focused on its potential industrial applications. Making long-lasting electrodes on a wide scale is the first step in academic research and investigations in the real world. Several novel methods, such as roll-to-roll micro-gravure printing, are needed to prepare usable industrial electrodes.

(iv) Improving the materials quality, elucidating the processes and ideal crystallization, and developing strategies to use COFs at a practical level, as free-standing films, and other usable forms are all challenges that still need to be overcome, despite the fact that the COF area has been focused on expanding the link between science and engineering and pinpointing features of practical importance. As a result, more fundamental considerations requiring substantial attention due to the modularity provided by COF design techniques are urgently required.

Finally, the critical examination of the significance of COF as multifunctional materials for usage in a wide range of applications is presented in-depth, along with the expected consequences and future directions. To that end, this review paper will serve as the first step in providing novel details on the production of COF-based materials and their potential applications in environmental, and engineering fields.

References

1. N. Gaur, D. Dutta, A. Jaiswal, R. Dubey and D. V. Kamboj, *Persistent Organic Pollutants (POPs): Monitoring, Impact and Treatment* (2022).
2. X. Wang, D. Sun and T. Yao, *Sci. China Earth Sci.* **59**, 1899 (2016).
3. B. Streit, *Experientia* **48**, 955 (1992).
4. Q. Qing Li, A. Loganath, Y. Seng Chong, J. Tan and J. Philip Obbard, *J. Toxicol. Environ. Health A* **69**, 1987 (2006).
5. M. V. Berghe, L. Weijs, S. Habran, K. Das, C. Bugli, S. Pillet, J.-F. Rees, P. Pomeroy, A. Covaci and C. Debier, *Environ. Res.* **120**, 18 (2013).
6. F. M. Van Dolah, M. G. Neely, L. E. McGeorge, B. C. Balmer, G. M. Ylitalo, E. S. Zolman, T. Speakman, C. Sinclair, N. M. Kellar and P. E. Rosel, *PLoS One*, **10**, e0130934 (2015).
7. K. C. Jones, *Environ. Sci. Technol.* **55**, 9400 (2021).
8. H. Furukawa and O. M. Yaghi, *J. Am. Chem. Soc.* **131**, 8875 (2009).
9. S. Y. Ding and W. Wang, *Chem. Soc. Rev.* **42**, 548 (2013).
10. H. Xu, J. Gao and D. Jiang, *Nat. Chem.* **7**, 905 (2015).
11. M. W. Powner, B. Gerland and J. D. Sutherland, *Nature* **459**, 239 (2009).
12. D.-M. Li, S.-Y. Zhang, J.-Y. Wan, W.-Q. Zhang, Y.-L. Yan, X.-H. Tang, S.-R. Zheng, S.-L. Cai and W.-G. Zhang, *CrystEngComm* **23**, 3594 (2021).
13. J.-P. Zhang, Y.-B. Zhang, J.-B. Lin and X.-M. Chen, *Chemical Rev.* **112**, 1001 (2012).
14. S. Kitagawa, *Chem. Soc. Rev.* **43**, 5415 (2014).
15. J. Jiang, Y. Zhao and O. M. Yaghi, *J. Am. Chem. Soc.* **138**, 3255 (2016).
16. H. M. El-Kaderi, J. R. Hunt, J. L. Mendoza-Cortés, A. P. Côté, R. E. Taylor, M. O'Keeffe and O. M. Yaghi, *Science* **316**, 268 (2007).
17. J. R. Hunt, C. J. Doonan, J. D. LeVangie, A. P. Côté and O. M. Yaghi, *J. Am. Chem. Soc.* **130**, 11872 (2008).

18. J. Tan, S. Namuangruk, W. Kong, N. Kungwan, J. Guo and C. Wang, *Ange. Chem. Int. Ed.* **55**, 13979 (2016).
19. C. Wu, Y. Liu, H. Liu, C. Duan, Q. Pan, J. Zhu, F. Hu, X. Ma, T. Jiu and Z. Li, *J. Am. Chem. Soc.* **140**, 10016 (2018).
20. P. Das, Q. Fu, X. Bao and Z.-S. Wu, *J. Mater. Chem. A* **6**, 21747 (2018).
21. M. Velický and P. S. Toth, *Appl. Mater. Today* **8**, 68 (2017).
22. H. Zhang, *Chem. Rev.* **118**, 6089 (2018).
23. N. Huang, P. Wang and D. Jiang, *Nat. Rev. Mater.* **1**, 16068 (2016).
24. K. Dey, M. Pal, K. C. Rout, S. Kunjattu, A. Das, R. Mukherjee, U. K. Kharul and R. Banerjee, *J. Am. Chem. Soc.* **139**, 13083 (2017).
25. A. P. Côté, A. I. Benin, N. W. Ockwig, M. O'Keeffe, A. J. Matzger and O. M. Yaghi, *Science* **310**, 1166 (2005).
26. R. Chen, J.-L. Shi, Y. Ma, G. Lin, X. Lang and C. Wang, *Angew. Chem. Int. Ed.* **58**, 6430 (2019).
27. R. Wang, W. Kong, T. Zhou, C. Wang and J. Guo, *Chem. Commun.* **57**, 331 (2021).
28. J. Guo, Y. Xu, S. Jin, L. Chen, T. Kaji, Y. Honsho, M. A. Addicoat, J. Kim, A. Saeki, H. Ihee, S. Seki, S. Irle, M. Hiramoto, J. Gao and D. Jiang, *Nat. Commun.* **4**, 2736 (2013).
29. S. Wei, F. Zhang, W. Zhang, P. Qiang, K. Yu, X. Fu, D. Wu, S. Bi and F. Zhang, *J. Am. Chem. Soc.* **141**, 14272 (2019).
30. S. J. Lyle, T. M. Osborn Popp, P. J. Waller, X. Pei, J. A. Reimer and O. M. Yaghi, *J. Am. Chem. Soc.* **141**, 11253 (2019).
31. S. Dalapati, S. Jin, J. Gao, Y. Xu, A. Nagai and D. Jiang, *J. Am. Chem. Soc.* **135**, 17310 (2013).
32. C. Qian, W. Zhou, J. Qiao, D. Wang, X. Li, W. L. Teo, X. Shi, H. Wu, J. Di, H. Wang, G. Liu, L. Gu, J. Liu, L. Feng, Y. Liu, S. Y. Quek, K. P. Loh and Y. Zhao, *J. Am. Chem. Soc.* **142**, 18138 (2020).
33. H. L. Nguyen, C. Gropp and O. M. Yaghi, *J. Am. Chem. Soc.* **142**, 2771 (2020).
34. G. Zhan, Z.-F. Cai, M. Martínez-Abadía, A. Mateo-Alonso and S. De Feyter, *J. Am. Chem. Soc.* **142**, 5964 (2020).
35. Z. Xiang and D. Cao, *J. Mater. Chem. A* **1**, 2691 (2013).
36. E. Jin, J. Li, K. Geng, Q. Jiang, H. Xu, Q. Xu and D. Jiang, *Nat. Commun.* **9**, 4143 (2018).
37. X. Chen, M. Addicoat, S. Irle, A. Nagai and D. Jiang, *J. Am. Chem. Soc.* **135**, 546 (2013).
38. X. Feng, X. Ding and D. Jiang, *Chem. Soc. Rev.* **41**, 6010 (2012).
39. J. Wang and S. Zhuang, *Coord. Chem. Rev.* **400**, 213046 (2019).
40. P. Kuhn, M. Antonietti and A. Thomas, *Angew. Chem. Int. Ed.* **47**, 3450 (2008).
41. B. P. Biswal, S. Chandra, S. Kandambeth, B. Lukose, T. Heine and R. Banerjee, *J. Am. Chem. Soc.* **135**, 5328 (2013).
42. C. O. Kappe, *Angew. Chem. Int. Ed.* **43**, 6250 (2004).
43. K. D. Zhang and S. Matile, *Ange. Chem. Int. Ed.* **54**, 8980 (2015).
44. Y. Jin, C. Yu, R. J. Denman and W. Zhang, *Chem. Soc. Rev.* **42**, 6634 (2013).
45. Y. Jin, Q. Wang, P. Taynton and W. Zhang, *Acc. Chem. Res.* **47**, 1575 (2014).
46. X. Feng, X. Zhuang, W. Zhao, F. Zhang, Y. Cao, F. Liu and S. Bia, *Poly. Chem.* **7**, 4176 (2016).
47. X. Liu, D. Huang, C. Lai, G. Zhang and L. Qin, H. Wang, H. Yi, B. Li, S. Liu, M. Zhang, R. Deng, *Chem. Soc. Rev.* **48**, 5266 (2019).
48. L. Xu, S.-Y. Ding, J. Liu, J. Sun, W. Wang and Q.-Y. Zheng, *Chem. Commun.* **52**, 4706 (2016).
49. N. L. Campbell, R. Clowes, L. K. Ritchie and A. I. Cooper, *Chem. Mater.* **21**, 204 (2009).
50. L. K. Ritchie, A. Trewin, A. Reguera-Galan, T. Hasell and A. I. Cooper, *Micropor. Mesopor. Mater.* **132**, 132 (2010).
51. S. Ren, M. J. Bojdys, R. Dawson, A. Laybourn, Y. Z. Khimyak, D. J. Adams and A. I. Cooper, *Adv. Mater.* **24**, 2357 (2012).
52. X. Guan, Y. Ma, H. Li, Y. Yusran, M. Xue, Q. Fang, Y. Yan, V. Valtchev and S. Qiu, *J. Am. Chem. Soc.* **140**, 4494 (2018).
53. B. P. Biswal, S. Chandra, S. Kandambeth, B. Lukose, T. Heine and R. Banerjee, *J. Am. Chem. Soc.* **135**, 5328 (2013).
54. E. M. Johnson, R. Haiges and S. C. Marinescu, *ACS Appl. Mater. Interf.* **10**, 37919 (2018).
55. P. G. Cozzi, *Chem. Soc. Rev.* **33**, 410 (2004).
56. W. J. Youngs, C. A. Tessier and J. D. Bradshaw, *Chem. Rev.* **99**, 3153 (1999).
57. J. Sedó, J. Saiz-Poseu, F. Busqué and D. Ruiz-Molina, *Adv. Mater.* **25**, 653 (2013).
58. J. Wang, X. Yang, T. Wei, J. Bao, Q. Zhu and Z. Dai, *ACS Appl. Bio Mater.* **1**, 382 (2018).
59. I. Ahmed and S. H. Jhung, *Coord. Chem. Rev.* **441**, 213989 (2021).
60. D. K. Yoo, B. N. Bhadra and S. H. Jhung, *J. Hazard. Mater.* **403**, 123655 (2021).
61. I. Ahmed, M. M. H. Mondol, H. J. Lee and S. H. Jhung, *Chem. Asian J.* **16**, 185 (2021).
62. L. Merí-Bofí, S. Royuela, F. Zamora, M. L. Ruiz-González, J. L. Segura, R. Muñoz-Olivas and M. J. Mancheño, *J. Mater. Chem. A* **5**, 17973 (2017).
63. N. Huang, R. Krishna and D. Jiang, *J. Am. Chem. Soc.* **137**, 7079 (2015).

64. H. Guo, J. Wang, Q. Fang, Y. Zhao, S. Gu, J. Zheng and Y. Yan, *Cryst. Eng. Comm.* **19**, 4905 (2017).
65. Y. Hu, N. Dunlap, S. Wan, S. Lu, S. Huang, I. Sellinger, M. Ortiz, Y. Jin, S.-H. Lee and W. Zhang, *J. Am. Chem. Soc.* **141**, 7518 (2019).
66. D.-G. Wang, N. Li, Y. Hu, S. Wan, M. Song, G. Yu, Y. Jin, W. Wei, K. Han, G.-C. Kuang and W. Zhang, *ACS Appl. Mater. Interf.* **10**, 42233 (2018).
67. R. P. Bisbey and W. R. Dichtel, *ACS Cent. Sci.* **3**, 533 (2017).
68. K. Dey, S. Mohata and R. Banerjee, *ACS Nano* **15**, 12723 (2021).
69. S. Karak, S. Kumar, P. Pachfule and R. Banerjee, *J. Am. Chem. Soc.* **140**, 5138 (2018).
70. F. Haase and B. V. Lotsch, *Chem. Soc. Rev.* **49**, 8469 (2020).
71. S. Karak, S. Kandambeth, B. P. Biswal, H. S. Sasmal, S. Kumar, P. Pachfule and R. Banerjee, *J. Am. Chem. Soc.* **139**, 1856 (2017).
72. D. Rodríguez-San-Miguel, C. Montoro and F. Zamora, *Chem. Soc. Rev.* **49**, 2291 (2020).
73. S. Wang, Z. Zhang, H. Zhang, A. G. Rajan, N. Xu, Y. Yang, Y. Zeng, P. Liu, X. Zhang, Q. Mao, Y. He, J. Zhao, B.-G. Li, M. S. Strano and W.-J. Wang, *Matter* **1**, 1592 (2019).
74. S. Wan, J. Guo, J. Kim, H. Ihee and D. Jiang, *Angew. Chem. Int. Ed.* **48**, 5439 (2009).
75. E. L. Spitler and W. R. Dichtel, *Nat. Chem.* **2**, 672 (2010).
76. M. Hao, Z. Chen, H. Yang, G. I. Waterhouse, S. Ma and X. Wang, *Sci. Bull.* **67**, 924 (2022).
77. R. Wen, Y. Li, M. Zhang, X. Guo, X. Li, X. Li, J. Han, S. Hu, W. Tan and L. Ma, *J. Hazard. Mater.* **358**, 273 (2018).
78. Z. You, N. Zhang, Q. Guan, Y. Xing, F. Bai and L. Sun, *J. Inorg. Organometall. Polym. Mater.* **30**, 1966 (2020).
79. Q. Shili, H. Xudong, J. Fenglong, W. Ying, C. Hongtao, H. Shuang, S. Yangyang and G. Lidi, *RSC Adv.* **12**, 18784 (2022).
80. Y. Xiao, C. Ma, Z. Jin, J. Wang, L. He, X. Mu, L. Song and Y. Hu, *Chem. Eng. J.* **421**, 127837 (2021).
81. Y. Li, H. Zhang, Y. Chen, L. Huang, Z. Lin and Z. Cai, *ACS Appl. Mater. Interf.* **11**, 22492 (2019).
82. S.-Y. Hu, Y.-N. Sun, Z.-W. Feng, F.-O. Wang and Y.-K. Lv, *Chemosphere* **286**, 131646 (2022).
83. X. Feng, L. Liu, Y. Honsho, A. Saeki, S. Seki, S. Irle, Y. Dong, A. Nagai and D. Jiang, *Angew. Chem. Int. Ed.* **51**, 2618 (2012).
84. Z. Xiao, Y. Zhou, X. Xin, Q. Zhang, L. Zhang, R. Wang and D. Sun, *Macromol. Chem. Phys.* **217**, 599 (2016).
85. S.-W. Lv, J.-M. Liu, C.-Y. Li, N. Zhao, Z.-H. Wang and S. Wang, *Chemosphere* **243**, 125378 (2020).
86. Y. Yao, Y. Hu, H. Hu, L. Chen, M. Yu, M. Gao and S. Wang, *J. Colloid Interface Sci.* **554**, 376 (2019).
87. C. Sun, L. Karuppasamy, L. Gurusamy, H.-J. Yang, C.-H. Liu, J. Dong and J. J. Wu, *Separ. Purif. Technol.* **271**, 118873 (2021).
88. Z.-Y. Choong, K.-Y. A. Lin and W.-D. Oh, *Mater. Lett.* **285**, 129079 (2021).
89. W. Wang, S. Deng, L. Ren, D. Li, W. Wang, M. Vakili, B. Wang, J. Huang, Y. Wang and G. Yu, *ACS Appl. Mater. Interface* **10**, 30265 (2018).
90. Y. Li, C.-X. Yang and X.-P. Yan, *Chem. Commun.* **53**, 2511 (2017).
91. F.-F. Li, W.-R. Cui, W. Jiang, C.-R. Zhang, R.-P. Liang and J.-D. Qiu, *J. Hazard. Mater.* **392**, 122333 (2020).
92. S. Mondal, S. Chatterjee, S. Mondal and A. Bhaumik, *ACS Sustain.Chem. Eng.* **7**, 7353 (2019).
93. S. G. Akpe, I. Ahmed, P. Puthiaraj, K. Yu and W.-S. Ahn, *Micropor. Mesopor. Mater.* **296**, 109979 (2020).
94. Y. Liang, L. Feng, X. Liu, Y. Zhao, Q. Chen, Z. Sui and N. Wang, *Chem. Eng. J.* **404**, 127095 (2021).
95. X. Zhu, S. An, Y. Liu, J. Hu, H. Liu, C. Tian, S. Dai, X. Yang, H. Wang, C. W. Abney and S. Dai, *AIChE J.* **63**, 3470 (2017).
96. R.-Q. Wang, X.-B. Wei and Y.-Q. Feng, *Chem. Eur. J.* **24**, 10979 (2018).
97. I. Ahmed and S. H. Jhung, *Coord. Chem. Rev.* **441**, 213989 (2021).
98. K. Dey, M. Pal, K. C. Rout, S. Kunjattu, A. Das, R. Mukherjee, U. K. Kharul and R. Banerjee, *J. Am. Chem. Soc.* **139**, 13083 (2017).
99. W. Zhang, L. Zhang, H. Zhao, B. Li and H. Ma, *J. Mater. Chem. A* **6**, 13331 (2018).
100. R. Wang, X. Shi, A. Xiao, W. Zhou and Y. Wang, *J. Membr. Sci.* **566**, 197 (2018).
101. S. Kandambeth, B. P. Biswal, H. D. Chaudhari, K. C. Rout, S. Kunjattu, H. S. Mitra, S. Karak, A. Das, R. Mukherjee, U. K. Kharul and R. Banerjee, *Adv. Mater.* **29**, 1603945 (2017).
102. F. Pan, W. Guo, Y. Su, N. A. Khan, H. Yang and Z. Jiang, *Sep. Purif. Technol.* **215**, 582 (2019).
103. L. M. Salonen, S. R. Pinela, S. P. Fernandes, J. Louçano, E. Carbó-Argibay, M. P. Sarriá, C. Rodríguez-Abreu, J. Peixoto and B. Espiña, *J. Chromatogr. A* **1525**, 17 (2017).
104. M. Gao, Q. Fu, M. Wang, K. Zhang, J. Zeng, L. Wang, Z. Xia and D. Gao, *Analyt. Chim. Acta* **1084**, 21 (2019).
105. W. Wang, S. Deng, L. Ren, D. Li, W. Wang, M. Vakili, B. Wang, J. Huang, Y. Wang and G. Yu, *ACS Appl. Mater. Interf.* **10**, 30265 (2018).

106. J. Huo, B. Luo and Y. Chen, *ACS Omega* **4**, 22504 (2019).
107. Y. Li, W. Chen, W. Hao, Y. Li and L. Chen, *ACS Appl. Nano Mater.* **1**, 4756 (2018).
108. Y. Hou, X. Zhang, C. Wang, D. Qi, Y. Gu, Z. Wang and J. Jiang, *New J. Chem.* **41**, 6145 (2017).
109. S. Zhuang, R. Chen, Y. Liu and J. Wang, *J. Hazard. Mater.* **385**, 121596 (2020).
110. H. Fan, J. Gu, H. Meng, A. Knebel and J. Caro, *Angew. Chem. Int. Ed.* **57**, 4083 (2018).
111. X. Zhang, H. Li, J. Wang, D. Peng, J. Liu and Y. Zhang, *J. Membr. Sci.* **581**, 321 (2019).
112. G. Kong, J. Pang, Y. Tang, L. Fan, H. Sun, R. Wang, S. Feng, Y. Feng, W. Fan, W. Kang, H. Guo, Z. Kang and D. Sun, *J. Mater. Chem. A* **7**, 24301 (2019).
113. G.-H. Ning, Z. Chen, Q. Gao, W. Tang, Z. Chen, C. Liu, B. Tian, X. Li and K. P. Loh, *J. Am. Chem. Soc.* **139**, 8897 (2017).
114. S. Kandambeth, B. P. Biswal, H. D. Chaudhari, K. C. Rout, S. Kunjattu, H. S. Mitra, S. Karak, A. Das, R. Mukherjee, U. K. Kharul and R. Banerjee, *Adv. Mater.* **29**, 1603945 (2017).
115. Z. Chen, Y. Li, Y. Cai, S. Wang, B. Hu, B. Li, X. Ding, L. Zhuang and X. Wang, *Carbon Res.* **2**, 8 (2023).
116. G. Cheng, A. Zhang, Z. Zhao, Z. Chai, B. Hu, B. Han, Y. Aix and X. Wang, *Sci. Bull.* **66**, 1994 (2021).
117. J. Kaleta, M. Kida, P. Koszelnik, D. Papciak, A. Puszkarewicz and B. Tchórzewska-Cieślak, *Arch. Environ. Prot.* **43**, 32 (2017).
118. D. Papciak, J. Kaleta, A. Puszkarewicz and B. Tchórzewska-Cieślak, *J. Ecol. Eng.* **17**, 119 (2016).
119. H.-C. Kim and M.-J. Yu, *J. Hazard. Mater.* **143**, 486 (2007).
120. X. Zhong, Z. Lu, W. Liang and B. Hu, *J. Hazard. Mater.* **393**, 122353 (2020).
121. G. Liu, Z. Dai, X. Liu, R. A. Dahlgren and J. Xu, *Carbon Res.* **1**, 1 (2022).
122. X. Liu, G. Verma, Z. Chen, B. Hu, Q. Huang, H. Yang, S. Ma and X. Wang, *Innovation* **3**, 100281 (2022).
123. L. Huang, M. He, B. Chen and B. Hu, *Chemosphere* **199**, 435 (2018).
124. M. Dinari and M. Hatami, *J. Environ. Chem. Eng.* **7**, 102907 (2019).
125. Y. Cai, Y. Jiang, L. Feng, Y. Hua, H. Liu, C. Fan, M. Yin, S. Li, X. Lv and H. Wang, *Anal. Chim. Acta* **1057**, 88 (2019).
126. Y. Zhao, K. X. Yao, B. Teng, T. Zhang and Y. Han, *Energy Environ. Sci.* **6**, 3684 (2013).
127. Y. Lan, X. Han, M. Tong, H. Huang, Q. Yang, D. Liu, X. Zhao and C. Zhong, *Nat. Commun.* **9**, 5274 (2018).